



Principals of simulation of ultrafast charge transfer in solution within the multichannel stochastic point-transition model[☆]



Alexey E. Nazarov, Roman G. Fedunov, Anatoly I. Ivanov^{*}

Volgograd State University, University Avenue 100, Volgograd 400062, Russia

ARTICLE INFO

Article history:

Received 14 July 2016

Received in revised form

14 September 2016

Accepted 19 September 2016

Available online 3 October 2016

Keywords:

Brownian trajectory

Surface hopping

Vibrational manifold

ABSTRACT

We introduce *bsmKinetic*, an implementation of the stochastic multichannel point-transition approach to simulation of the charge transfer kinetics in molecular systems with reorganization of many intramolecular high-frequency vibrational mode in solvents with several relaxation timescales. The software provides simulation of the charge transfer kinetics in the molecular systems with many electronic states involved in photochemical transformations. It also allows simulating the charge transfer occurring in both equilibrium and nonequilibrium regimes. *bsmKinetic* is open-source software distributed under the terms of the GPL without additional components. Software is implemented on multiple computing platforms. It exploits Matsumoto and Nishimura source code for pseudorandom number generator and a hierarchy of custom parallelization of the stochastic trajectories built on MPI.

Program summary

Program Title: *bsmKinetic*

Program Files doi: <http://dx.doi.org/10.17632/ywd9cwzzx9.1>

Licensing provisions: GPLv3

Programming language: C++

Supplementary material: MPI

Nature of problem: Simulation of dynamics and kinetics of charge transfer in solution.

Solution method: Brownian simulation method for diffusional dynamics, stochastic point-transition approach for electronic and vibronic transitions.

Additional comments including Restrictions and Unusual features: Binary search of transition-points for each diffusion step on crosses of vibrational manifolds, initial electron-vibrational distribution includes pump pulses characteristics, classical description of the solvent fluctuations, description of the vibronic states in terms of populations ignoring the quantum coherence, usage of the diabatic basis, parabolic terms.

Reference:

- [1] M. Matsumoto, T. Nishimura Dynamic Creation of Pseudorandom Number Generators, in book Monte Carlo and Quasi-Monte Carlo Methods, 1998, Springer, 2000, 56–69.

© 2016 Elsevier B.V. All rights reserved.

[☆] This paper and its associated computer program are available via the Computer Physics Communication homepage on ScienceDirect (<http://www.sciencedirect.com/science/journal/00104655>).

^{*} Corresponding author.

E-mail address: Anatoly.Ivanov@volsu.ru (A.I. Ivanov).

<http://dx.doi.org/10.1016/j.cpc.2016.09.015>

0010-4655/© 2016 Elsevier B.V. All rights reserved.

1. Introduction

Electron transfer as one of the most widespread reaction in the nature plays a central role in many chemical, biological and physical processes [1–6]. It can occur on timescale covering huge area from seconds to few femtoseconds [7]. Such reactions are of primary importance in the emerging areas of molecular electronics, for example, dye/semiconductor systems applied in dye-sensitized solar cells [6,8,9]. Intensive investigations of

the thermal and photoinduced charge transfer kinetics by both experimental and theoretical methods during last few decades have led to deep understanding of the detailed mechanism of such reactions [1,4,10–13].

Modern femtosecond UV–Vis transient absorption spectroscopy provides possibility to explore ultrafast photoinduced processes occurring in the excited electronic states. The data obtained in transient absorption spectroscopy measurements comprise a large amount of potential information on the dynamics of the chemical transformations. Indeed, ultrafast spectroscopic technique allows observing many subtle details of ultrafast charge transfer. Among them: nonexponential charge transfer kinetics [14–16], effect of the excitation wavelength on the ultrafast charge recombination dynamics of donor–acceptor complexes in polar solvents [16], influence of intramolecular high-frequency vibrational mode excitation on ultrafast photoinduced charge transfer and charge recombination kinetics [17]. These experiments clearly show that the nonequilibrium of the nuclear subsystem in ultrafast photochemical processes can play a key role [17–22]. This requires the creation of the theory of elementary photoinduced processes including an explicit description of the processes of photoexcitation, probe, the evolution of the nuclear subsystem, and the chemical dynamics occurring in parallel with it. For this field of science this is especially important because the quantitative interpretation of the results obtained in the experiments is only possible within the framework of certain models [3]. The fact is that the measured pump–probe signal contains only indirect information on the dynamics of the reactant and product populations because in the transient spectra the chemical dynamics entangled with the intramolecular reorganization and surrounding medium relaxation.

Theory which meets these challenges has to describe the dynamics of a system with many degrees of freedom consisting of the electronic and nuclear subsystems of the reactants and products, as well as the surrounding solvent. One of the theories pretending to qualitatively describe many features of the ultrafast charge transfer kinetics is based on the multichannel stochastic point-transition model [19,23–27]. In the base of this model lies the Marcus concept of parabolic free energy surfaces constructed in space of solvent polarization coordinates. Classical motion of particles along these surfaces reflects reorganization of solvent in the course of electron transfer and is fully characterized by the solvent relaxation function that can be borrowed from data of independent experiments [28]. The reorganization of several (up to ten) intramolecular high-frequency vibrational modes is included in the model. The molecular system is described in terms of distribution functions along classical degrees of freedom for every quantum state. The number of the distribution functions can be as large as several thousands. Their evolution is determined by the set of diffusion-like equations. The dimension of the space is given by the number of the relaxation modes of the solvent and typically lies in the interval 2–4.

In this paper we introduce a computer code, named `bsmKinetic` to simulate ultrafast charge transfer kinetics in solution within the multichannel stochastic point-transition model, and which is being distributed under the terms of the GPL license [29], as the individual software. In Section 2 a minimal theoretical background is presented and some notations for the problem are established. An algorithm implemented in `bsmKinetic` to simulate diffusion motion of the solvent, electronic transitions (surface hoppings at electronic term intersections), vibrational relaxation, internal conversion are described in Section 3. Description of files, structure of source code, parallelization concept are presented in Section 4.

2. Minimal theoretical background

For description of typical experiments on kinetics of photoinduced electron transfer in polar solvents, a model should include several electronic states of the reactants and products, a number of the intramolecular high-frequency vibrational modes active in electronic transitions, solvent and its interaction with the solute as well as vibrational redistribution/relaxation of the system [19,30]. Dynamics of a polar solvent are characterized by relaxation function. The solvent relaxation function, $X(t)$, can be written in the form [31,32]

$$X(t) = \sum_{i=1}^N x_i e^{-t/\tau_i}, \quad \sum_{i=1}^N x_i = 1, \quad (1)$$

where x_i and τ_i are the weight and the relaxation time constant, respectively, N is the number of the solvent modes. Each summand of the relaxation function Eq. (1) is associated with different kinds of relaxation modes of the solvent. Every separate solvent relaxation mode is described in the terms of a solvent coordinate Q_i .

In the terms of the solvent coordinates, Q_i , a diabatic free energy surface of an electronic state $|q\rangle$ with its vibrationally excited sublevels, can be written in the form [33]

$$U_q^{(\vec{n})}(\mathbf{Q}) = \frac{1}{2} \sum_{i=1}^N \left(Q_i - \sqrt{2E_{rmi}^{qr}} \right)^2 + \Delta G^{qr} + \sum_{\alpha=1}^M n_{\alpha} \hbar \Omega_{\alpha}, \quad (2)$$

where \mathbf{Q} stands for the vector (Q_1, Q_2, \dots, Q_N) , $E_{rmi}^{qr} = x_i E_{rmi}^{qr}$ is the reorganization energy of the i th solvent mode, E_{rmi}^{qr} and ΔG^{qr} are the total reorganization energy of the medium and the free energy change between the $|q\rangle$ and reference $|r\rangle$ states, respectively, $\hbar \Omega_{\alpha} \gg k_B T$ is the frequency of the α th intramolecular high-frequency vibrational mode, k_B and T are the Boltzmann constant and the temperature, respectively, \hbar is the Planck constant, $n_{\alpha} = 0, 1, 2, \dots$ is the quantum numbers of the α th high-frequency mode, M is the number of high-frequency modes. The vector \vec{n} is a set of M quantum numbers $(n_1, n_2, \dots, n_{\alpha}, \dots, n_M)$. Each sublevel is associated with a set of quantum numbers. It is supposed that the origins of the free energy and the coordinates, Q_i , are placed at the minimum of the reference state ($|r\rangle$) term.

In the framework of the stochastic point-transition approach [22,26,33], the time evolution of the system is described by the equation for the probability distribution function for \vec{n} th sublevel of the $|q\rangle$ state, $\rho_q^{(\vec{n})}(\mathbf{Q}, t)$ [19],

$$\begin{aligned} \frac{\partial \rho_q^{(\vec{n})}}{\partial t} = & \hat{L}_q \rho_q^{(\vec{n})} + \sum_{\alpha} \left[\frac{\rho_q^{(\vec{n}'_{\alpha})}}{\tau_{v\alpha}^{(n_{\alpha}+1)}} - \frac{\rho_q^{(\vec{n})}}{\tau_{v\alpha}^{(n_{\alpha})}} \right] \\ & + \sum_{\vec{m}, r \neq q} K_{qr}^{\vec{n}\vec{m}} \left[\rho_r^{(\vec{m})} - \rho_q^{(\vec{n})} \right] + \sum_{r, \vec{m}} R_{qr}^{\vec{n}\vec{m}} \left[\rho_r^{(\vec{m})} - \rho_q^{(\vec{n})} \right], \quad (3) \end{aligned}$$

where \hat{L}_q is the Smoluchowski operators describing diffusion on the $U_q^{(\vec{n})}$ free energy surfaces,

$$\hat{L}_q = \sum_{i=1}^N \frac{1}{\tau_i} \left[1 + \left(Q_i - \sqrt{2E_{rmi}^{qr}} \right) \frac{\partial}{\partial Q_i} + k_B T \frac{\partial^2}{\partial Q_i^2} \right]. \quad (4)$$

The model, Eq. (3), includes single-quantum irreversible vibrational relaxation $n_{\alpha} \rightarrow n_{\alpha} - 1$ proceeding with the rate constant $1/\tau_{v\alpha}^{(n_{\alpha})}$, where $\tau_{v\alpha}^{(n_{\alpha})} = \tau_{v\alpha}/n_{\alpha}$, $\tau_{v\alpha}$ is the vibrational relaxation time constant [33]. The vector \vec{n}'_{α} differs from \vec{n} only by adding one vibrational quantum for the high-frequency α th mode that is $\vec{n}'_{\alpha} = (n_1, n_2, \dots, n_{\alpha} + 1, \dots, n_M)$.

Transitions between vibrational sublevels of $|q\rangle$ and $|r\rangle$ states are described by the Zusman parameters [19,28]

$$K_{qr}^{\bar{n}\bar{m}} = \frac{2\pi (V_{el}^{qr})^2 F_{\bar{n}\bar{m}}^{qr}}{\hbar} \delta(U_r^{(\bar{m})} - U_q^{(\bar{n})}), \quad (5)$$

$$U_r^{(\bar{m})} - U_q^{(\bar{n})} = Z^{qr} - Z_{\#}^{qr}, \quad (6)$$

$$F_{\bar{n}\bar{m}}^{qr} = \prod_{\alpha=1}^M \exp\{-S_{\alpha}^{qr}\} n_{\alpha}! m_{\alpha}! \times \left[\sum_{l=0}^{\min(n_{\alpha}, m_{\alpha})} \frac{(-1)^{m_{\alpha}-l} (\sqrt{S_{\alpha}^{qr}})^{n_{\alpha}+m_{\alpha}-2l}}{l!(n_{\alpha}-l)!(m_{\alpha}-l)!} \right]^2, \quad (7)$$

$$S_{\alpha}^{qr} = \frac{E_{rv\alpha}^{qr}}{\hbar\Omega_{\alpha}}, \quad (8)$$

where $Z^{qr} = \sum \sqrt{2E_{rmi}^{qr}} Q_i$ and $Z_{\#}^{qr} = E_{rim}^{qr} + \Delta G^{qr} + \sum n_{\alpha} \hbar\Omega_{\alpha}$ are the reaction coordinate and the intersection points between free energy curves along the reaction coordinate, respectively, V_{el}^{qr} is electronic coupling between $|q\rangle$ and $|r\rangle$ states, $E_{rv\alpha}^{qr}$ is the reorganization energy of the α th vibrational mode, $F_{\bar{n}\bar{m}}^{qr}$ and S_{α}^{qr} are the Franck–Condon and the Huang–Rhys factors, respectively. The matrix $R_{\bar{n}\bar{m}}^{qr}$ describes internal conversion. Usually internal conversion occurs between locally excited states of the donor or acceptor which can compete with ultrafast charge transfers. The energy conservation law requires the condition $U_q^{(\bar{n})} = U_r^{(\bar{m})}$ have to be met for internal conversion.

To describe quantitatively the chemical and physical transformations, the q th term population, $P_q(t)$, and a time-independent effective rate constant are often used

$$k_q^{-1} = \int_0^{t_0} P_q(t) dt, \quad P_q(t) = \sum_{\bar{n}} \int \rho_q^{(\bar{n})}(\mathbf{Q}, t) \prod dQ_i \quad (9)$$

where t_0 is the time interval of the population reduction down to minimal value (from 1% to 5%), which can be monitored in experiments. The initial distribution function is determined by the physical formulation of the problem. As a rule it is a thermal distribution at the lowest electronic state of the donor term or it is arbitrary distribution at the specified term, for example the excited state can be prepared by a laser pulse.

In the classical problem of two-level thermal electron transfer, the initial conditions can be written in the form

$$\rho_p^{(0)}(\mathbf{Q}, t=0) = 0, \quad (10)$$

$$\rho_r^{(0)}(\mathbf{Q}, t=0) = A \exp\left\{-\frac{U_r^{(0)}}{k_B T}\right\}, \quad (11)$$

where A —the normalization factor, r and p are the reactant and product states, correspondingly.

In the study of photoinduced electron transfer, initial condition of the excited state is formed by short laser pulse with the carrier frequency ω_e and the duration of excitation τ_e . The pump pulse is assumed to be of the Gaussian form

$$E(t) = E_0 \exp\left\{i\omega_e t - \frac{t^2}{\tau_e^2}\right\}. \quad (12)$$

The duration τ_e is short so that the solvent is considered to be frozen during excitation. All high-frequency vibrational modes are supposed initially to be in the ground state. The initial probability distribution function of excited state can be written in the following

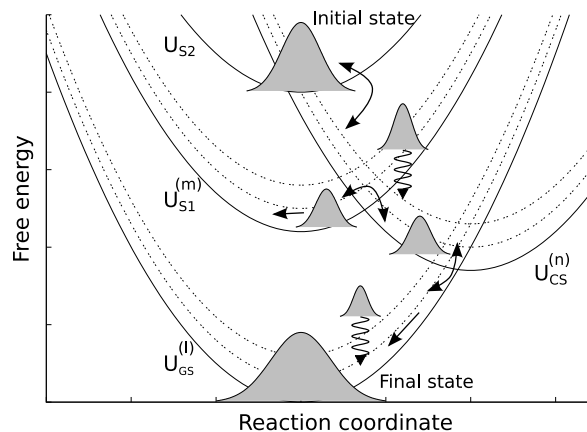


Fig. 1. Cuts in the free energy surface of the ground, first and second excited states, and the CS state. The dashed lines are the vibrational sublevels of the CS, GS, and S_1 electronic states. Reversible transitions are shown by double sided arrows. Solvent relaxation is shown by single sided arrows. Vibrational relaxation is shown by wave arrows.

general form [22]

$$\rho_e^{(\bar{n})}(\mathbf{Q}, t=0) = AP_{\bar{n}} \exp\left\{-\frac{(\hbar\delta\omega_e^{(\bar{n})} - (U_e^{(\bar{n})} - U_g^{(0)}))^2 \tau_e^2}{2\hbar^2} - \frac{U_g^{(0)}}{k_B T}\right\}, \quad (13)$$

$$P_{\bar{n}} = \prod_{\alpha} \frac{(S_{\alpha}^{eg})^{n_{\alpha}}}{n_{\alpha}!} \exp\{-S_{\alpha}^{eg}\}, \quad (14)$$

where A is the normalization factor, $\hbar\delta\omega_e^{(\bar{n})} = E_{rim}^{eg} + \Delta G^{eg} - \sum n_{\alpha} \hbar\Omega_{\alpha} + \hbar\omega_e$, $P_{\bar{n}}$ is the Franck–Condon factor at the excitation stage. In general a number of wave packets simultaneously appear on different vibrational sublevels of the excited state.

At the end of this section we describe a model incorporating the four electronic states with vibrational sublevels. The excitation of the system from the ground state to the state S_2 leads to appearance of a wave packet in the vicinity of the S_2 term bottom (see Fig. 1). Further two competing processes proceed. The first is the internal conversion $S_2 \rightarrow S_1$ (not shown in Fig. 1) and the second is the charge separation at the points of the term crossings $U_{S2} = U_{CS}$ to populate the vibrational sublevels of the CS state (dashed lines in Fig. 1). Next, the systems created in the CS state at the term crossing points move to the $U_{CS}^{(\bar{n})}$ term minimum due to the medium relaxation (straight single sided arrows in Fig. 1). During the medium relaxation, the systems pass the crossing points of the terms $U_{S1}^{(\bar{m})}$ and $U_{CS}^{(\bar{n})}$ that results in hot transitions to the first excited state S_1 (curved double sided arrow in Fig. 1). In parallel with the hot transitions the intramolecular vibrational relaxation occurs that is imagined as vertical transitions between neighbor sublevels (wavy arrow in Fig. 1).

Although, many features of experimental kinetics can be reproduced by using formal kinetic treatment nevertheless the stochastic model provides considerable advantages. Firstly, the stochastic model allows simulating the kinetics based on the known values of the physical parameters of the system (reorganization energies, free energy gaps, electronic couplings, vibrational frequencies, dynamic parameters of the solvents and others) that can be determined in independent experiments. As a result, there are correlations between the rate constants of different stages because they are determined at least partly by the same parameters. Contrary to this the formal kinetics consider the rate constants to be free parameters. Secondly, the approach of formal kinetics is applicable only when the reactions proceed in the kinetic mode, that is,

the nuclear subsystem is close to its equilibrium state while the stochastic model can describe even strongly nonequilibrium reactions. This is especially important for ultrafast reactions that typically includes strongly nonequilibrium stages.

3. Algorithm

A set of the probability distribution functions $\rho_q^{(\vec{n})}(\mathbf{Q}, t)$ plays the central role in the considered problem. The function $\rho_q^{(\vec{n})}(\mathbf{Q}, t)$ allows calculating different physical characteristics of practical interest, for example: state populations, quantum yields, reaction rate constants. The description of the ensemble evolution can be given in the terms of Brownian particle packet. Motion of a particle is characterizes by a stochastic trajectory. It can be calculated by using the stochastic algorithm [34]. In what follows we describe each process included in Eq. (3) in detail.

3.1. Diffusion

At the base of the stochastic algorithm lies the Green's function $G_q(\mathbf{Q}, t, |\mathbf{Q}_0\rangle) = \prod_i G_q(Q_i, t, |Q_{0i}\rangle)$ which describes an evolution of particle distribution on the parabolic term $U_q^{(\vec{n})}$. It is the solution of the one-dimensional diffusion equation $\hat{L}_{qi}G_q(Q_i, t, |Q_{0i}\rangle) = 0$ with the initial condition $G_q(Q_i, t = 0, |Q_{0i}\rangle) = \delta(Q_i - Q_{0i})$

$$G_q(Q_i, t, |Q_{0i}\rangle) = \frac{1}{\sqrt{2\pi\sigma_i^2(t)}} \exp\left\{-\frac{(Q_i - M_i(Q_{0i}, t))^2}{2\sigma_i^2(t)}\right\}, \quad (15)$$

$$M_i(Q_{0i}, t) = \sqrt{2E_{rmi}^{qr}} + (Q_{0i} - \sqrt{2E_{rmi}^{qr}})e^{-t/\tau_i}, \quad (16)$$

$$\sigma_i^2(t) = k_B T (1 - e^{-2t/\tau_i}). \quad (17)$$

We have presented the diffusion description based on the distribution functions. There is an alternative but equivalent description in the terms of Langevin equation that deals with stochastic trajectories known also as the Brownian trajectories. The Green function Eq. (15) allows connecting these two approaches. Since the packet conserves the Gauss form under the evolution on the parabolic surface with the mean value for i th coordinate, $M_i(Q_{0i}, t)$, and the dispersion, $\sigma_i(t)$, the Brownian trajectory is [34]

$$Q_i^{(k+1)} = M_i(Q_i^{(k)}, \Delta t_k) + \sigma_i(\Delta t_k)X^{(k)}, \quad (18)$$

where $\Delta t_k = t_{k+1} - t_k$ is a small time interval, $Q_i^{(k)}$ is a particle coordinate on k th time step, $X^{(k)}$ is the Gaussian random number with zero mean value and unit dispersion.

3.2. Transitions

A particle on the k th step can change its state due to hopping between electronic terms, vibrational relaxation, and internal conversion. The survival probability for each type of transitions is calculated by the equation

$$S(t_{k+1}) = \exp\left\{-\int_{t_k}^{t_{k+1}} K(t') dt'\right\}, \quad (19)$$

where $K(t)$ can be one of the next rates $K_{qr}^{\vec{n}\vec{m}}(Z^{qr}(t))$, $1/\tau_{v\alpha}^{(n_\alpha)}$, $R_{qr}^{\vec{n}\vec{m}}$.

3.2.1. Hoppings

Calculating the integral in Eq. (19) with $K(t) = K_{qr}^{\vec{n}\vec{m}}(Z^{qr}(t))$, the survival probability for single crossing is written in the form [22]

$$S_h(t_{k+1}) = \exp\left\{-\frac{2\pi(V_{el}^{qr})^2 F_{\vec{n}\vec{m}}^{qr} \Delta t_k}{\hbar(Z_{k+1}^{qr} - Z_k^{qr})}\right\}. \quad (20)$$

Obviously, a particle passes through term crossings on the k th step if the condition $Z_{\#}^{qr} \in (Z_k^{qr}, Z_{k+1}^{qr})$ is met. The total number of the crossings between two electronic terms can be very large because of manifold of the vibrational sublevels. To find a set of crossings for Δt_k interval (so called k th set) a binary search algorithm is used. Since the total probability of electronic transitions at the k th step is small, it is the sum of the probabilities of transitions into specific states. In this case the single term intersection from the set can be randomly selected. To simulate a hopping event a random number χ of uniform distribution on the interval $[0, 1]$ is compared with the hopping survival probability S_h . If $S_h < \chi$ then the particle turns on the other term, else the crossing is randomly selected again. The number of repetitions cannot exceed the size of the k th set. As well transitions between multiple electronic states $|q\rangle \rightarrow |r\rangle$, where q is fixed and $r = 0, 1, \dots, N$, can be realized by the N repetition of a random selection of the pairs $(q, 1), (q, 2), \dots, (q, N)$.

3.2.2. Vibrational relaxation

The particle in an excited vibrational sublevel with the energy $U_q^{\vec{n}'}$, has a non-zero probability of transition to the lower sublevel with the energy $U_q^{\vec{n}}$. Using $K(t) = 1/\tau_{v\alpha}^{(n_\alpha)}$, the survival probability of a particle with α th quantum on the k th step is calculated by

$$S_v(t_k) = \exp\left\{-\frac{n_\alpha \Delta t_k}{\tau_\alpha}\right\}. \quad (21)$$

The α th value is randomly selected from the vector $\vec{n}' = (n_1, n_2, \dots, n_\alpha + 1, \dots, n_M)$ M times. A simulation of vibrational transition to the lower sublevel determined by the vector $\vec{n} = (n_1, n_2, \dots, n_\alpha, \dots, n_M)$ includes a generation of a new χ and comparison $S_v < \chi$.

3.2.3. Internal conversion

Internal conversion can play important role in photochemical processes. It is included in the stochastic algorithm as a particle transition from $U_q^{\vec{n}}$ to $U_r^{\vec{m}}$ that is possible at the following condition $U_q^{\vec{n}} \geq U_r^{\vec{m}}$. This procedure is applicable for transitions with $E_{rm}^{qr} = 0$. Using $K(t) = R_{qr}^{\vec{n}\vec{m}} = 1/\tau_{ic}^{qr}$, the conversion survival probability of a particle is calculated by

$$S_c(t_k) = \exp\left\{-\frac{\Delta t_k}{\tau_{ic}^{qr}}\right\}, \quad (22)$$

where τ_{ic}^{qr} is the internal conversion time constant. Simulation of internal conversion event consists of a generation of new χ and comparison $S_c < \chi$.

3.3. Summary

Assuming all of the above processes are independent of each other, the type of particle transition has a random character. General algorithm for N particles is:

1. The particle state $\{\mathbf{Q}, q, n\}$ on the current time step is determined.
2. The new particle coordinates Q are calculated (see Section 3.1).
3. The (q, r) pair is played out and the reaction coordinate Z^{qr} is calculated.
4. The transitions are played out (see Section 3.2).
5. Repeat items 3, 4 N times.
6. Go to the next time step.

The distribution on a sublevel, $\rho_q^{(\vec{n})}(\mathbf{Q}, t)$, is formed by a large set of particles. Initialization of the state $\{Q, q, n\}$ in zero time is performed by a random number generation with the distribution from Eq. (11) or (13).

4. Description and usage of software

4.0.1. Files

A model of charge transfer from the second excited state is used to illustrate the possibilities of the software. The model involves four electronic states as well as their vibrational sublevels and transitions between them (see Fig. 1). The model is rather realistic and is able quantitatively describe complex nonequilibrium dynamics observed in the electron transfer from the second excited state in Zn-porphyrin-imide dyads [26].

The executable file `bsmKinetic` performs the stochastic simulation and calculates the kinetics. The configuration file has text format and arbitrary name. This name is a single argument to the program. If the argument is not specified, the program generates a configuration example and runs it. This example contains a model incorporating four electronic states (the first and the second singlet excited, the charge separated, and the ground states) as well as their vibrational sublevels for the computation of kinetics of the charge separated state population. The kinetics of all four electronic state is written to `bsm_term_populations.txt`. The first column is the current time, the second and following columns are the term populations. The term numeration is specified from 0 to 3 (0—the second singlet excited, 1—the first singlet excited, 2—the charge separated state, 3—the ground states). The kinetics of vibrational sublevels of term i is written to `bsm_subterms_of_termi.txt`. The information about the simulation progress and the rate constant Eq. (9) for the each state are written to `bsm_kinetics.txt`. Information about vibrational quanta of the first thousand of vibrational sublevels for a set of vibrational modes is written to `bsm_subterm_structure_of_termi.txt` (i runs from 0 to 3 in accordance with the term numbers). Information about the current state of the particles is written to the binary file `bsm_state_of_particles`. It is used to continue the system evolution and kinetics calculation. The file names generated by the program have a suffix in the form `_rvi_idj` (i is the number of the record version, j is the process identifier).

4.0.2. Structure of the configuration file

The configuration file contains groups in which the model parameters are initialized. Any group name begins with the character `$` and the group name is written with the capital letters. All groups in the file must be terminated by the keyword `$END`. Order of the groups is arbitrary. The group parameters are set in the following format, `keyword = value`. If a parameter is an array consisting of N elements, then the format keyword is `[value1, value2, ..., valueN]`. All keywords are case sensitive.

In the `$MAIN` group the dimension of the calculation space is determined. In the considered example the mandatory keywords are `numModes_c` for the number of solvent modes, `numModes_v` for the number of vibrational modes, `numTerms` for the number of electronic terms, `numPairs` for the number of term pairs between which there is an interaction, `numParticles` for the total number of the particles, `numTimeLayers` for the number of the time layers, `timeStart` and `timeEnd` for the time interval of the electron transfer evolution.

The type of numbered groups, `$GROUPNAMEi`, appears in the configuration file. The index i runs from 0 to $N - 1$, where N is the number specified in the `$MAIN` group. The group `$MAIN` involves the keyword `numModes_c = 3`. The configuration file must contain `$MODE_CO`, `$MODE_C1` and e.t.c. Similarly, the other groups appear. For DMF solution, the weights and relaxation time constants are [35] $x_1 = 0.508$, $x_2 = 0.453$, $x_3 = 0.039$, $\tau_1 = 0.217$ ps, $\tau_2 = 1.70$ ps, and $\tau_3 = 29.1$ ps. In

`$MODE_Ci` group the keywords `x` and `tau` are the i th weight and i th time relaxation constant. Intramolecular reorganization of phenylcyclopropane/tetracyanoethylene complex involves 5 active vibrational modes [26]. In the `$MODE_Vi` group the keywords `x`, `tau`, `omega`, `numQuantaMax`, are the i th weight, time relaxation constant, vibrational frequency (in the energy units) and the maximum number of the vibrational quanta. In the `$TERMi` group the keywords `DeltaG` and `Erm ≥ 0` specify the free energy change and the total reorganization energy of the relaxation modes relatively to the reference term. For convenience, the reference term can be determined by the conditions `DeltaG = 0` and `Erm = 0`. In the example considered the reference term is S_2 . The term positions are recalculated for each connected pair terms. In `$PAIRi` group the keyword-array `termsNo` determines the indexes of the terms constituting a pair. If there is a pair intersected terms and interaction between them then electronic coupling `Vel` keyword must be larger zero. If levels are not intersected then the `tau` keyword can be larger zero to specify internal conversion. Franck-Condon factors for a pair of terms are specified by the vibrational reorganization energy and its distribution among the vibrational modes through the keyword `Erv`. The `$SUBTERMS i` group is associated with i th term. It is not mandatory, but both keywords `isExistence`, `mcFLimiter` reduce the number of subterms to accelerate calculation. For example [26], the term S_2 does not contain the subterms and keyword `isExistence = 0`.

The initial distribution parameters are defined in unnumbered group `$INITDISTR_THERMAL`. The keyword `Erm` specifies the thermal distribution (see Eq. (11)) on the term defined by the keyword `termNo`. Alternatively, the initial distribution can be created on an arbitrary term by setting the pumping parameters in a group `$INITDISTR_PUMP`. The keyword `pairNo` is an index for pair which contains E_{rm}^{qr} , E_{rv}^{qr} , ΔG^{qr} . The keywords `x_c` and `x_v` are arrays of values that specify the i th parts E_{rm}^{qr} , E_{rv}^{qr} to classical and vibrational modes in the pumping process. The pump pulse parameters are set by keyword `tau` and `omega`. Note these groups are mutually exclusive.

The additional parameters governing time of simulation are included in the group `$KINETICS`. The keyword `numSTimeLayers` specifies the number of saved time layers to calculate and save populations. This key is need to reduce total time required for calculations average values of populations.

4.0.3. Structure of source code

`bsmKinetic` code is based on classes. Some classes are associated with physical objects of the electron transfer model. For example classical and vibrational modes are described in classes `Mode_c`, `Mode_v`. Pairs, terms and subterms are described in the classes with the same names. The most of the names of the class fields have the names similar to the group parameters in the configuration file. The class `Particles` incorporates methods which realize the algorithms of diffusion motion and transitions. All information about physical model from these classes is accumulated in the class `Environment`. The method `evolve` of the `Environment` class realizes cycle by time layers and accepts references to objects of classes `Particles` and `Calculator`. Abstract class `Calculator` contains virtual method `compute` that accepts index of time layer and references to class object of `Particles`. It can provide an alternative implementation for the some problems. In this source code the class `CalculatorKinetics` is a child of `Calculator`. Its method of `compute` both the population and rate constant.

4.0.4. Parallelization

Source code of `bsmKinetic` uses Message Passing Interface (MPI). The total number of particles is divided per processes in accordance with the specified weights in the configuration file. By default the number of the particles per a process is distributed uniformly. Data exchange between the host and the rest of the processes occurs in end of calculation.

To avoid correlation of random numbers between processes Mersenne Twister pseudorandom number generator (PRNG) in the realization of M. Matsumoto and T. Nishimura is used [36]. A seed of PRNG can be defined manually by in group `$MAIN` through keyword `seed` is equal to any integer value. If `seed` is equal to `-1` then `seed` is calculated in two steps. First step, PRNG from the library `<cstdlib>` is initialized by using the current time. Second step, seeds of Mersenne Twister is initialized by formula $(id+1) \cdot \text{rand}()$, where `id` is the identifier of the processes.

5. Comparison with an analytical solution and the grid method

To show the correctness of the algorithms used and their realization in the code the population dynamics obtained with stochastic simulations are compared with an exact analytical result. For a two-level system in a solvent with single relaxation mode and the relaxation time τ that described by the equations

$$\frac{\partial \rho_r}{\partial t} = \hat{L}_r \rho_r - \frac{2\pi V_n^2}{\hbar} [\rho_r - \rho_p^{(n)}] \delta(U_r - U_p^{(n)}), \quad (23)$$

$$\frac{\partial \rho_p^{(n)}}{\partial t} = \hat{L}_p \rho_p + \frac{2\pi V_n^2}{\hbar} [\rho_r - \rho_p^{(n)}] \delta(U_r - U_p^{(n)}) - \frac{\rho_p^{(n)}}{\tau_v^{(n)}}, \quad (24)$$

$$V_n^2 = V_{el}^2 \frac{S^n e^{-S}}{n!}, \quad (25)$$

$$\rho_r(t=0, Q) = A \exp \left\{ -\frac{(Q - \sqrt{2E_{rm}})^2}{2k_B T} \right\}, \quad (26)$$

the non-thermal transition probability, W_{NT} , after the wave packet passing through the term intersection has been analytically calculated [37].

Eq. (27) is an exact analytical solution for the two-state model described by Eqs. (23)–(26) provided the wave packet has totally passed the sink and the thermal transitions do not occur. These conditions determine the choice $t = 5\tau$. This guarantees that the tail of the wave packet above the sink is negligible and the role of the thermal transitions is minor. A variation of t around the selected value 5τ has a minor effect on the results.

$$W_{NT} = \frac{2\pi V_n^2}{A_r (1+g)} \quad (27)$$

where

$$g = 2\pi V_n^2 \left(\frac{1}{A_r} + \frac{1}{|A_p| f_v} \right), \quad f_v = \left[1 + \frac{8E_{rm} k_B T}{\tau \tau_v^{(n)} A_p^2} \right]^{1/2},$$

$$A_r = (\Delta G + n\hbar\Omega + E_{rm})/\tau, \quad A_p = (\Delta G + n\hbar\Omega - E_{rm})/\tau.$$

With the initial conditions Eq. (26), the wave packet practically totally passes the term intersection within time 5τ therefore the reactant population, $\rho_r(t = 5\tau)$, is compared with the quantity $1 - W_{NT}$ as a function of the electronic coupling for few values of the vibrational relaxation time, τ_v . Calculation are performed with the following parameters: $E_{rm} = 1.0$ eV, $\Delta G = 0.0$ eV, $E_{rv} = 0.3$ eV, $\hbar\Omega = 0.1$ eV, $\tau = 1$ ps, $n = 2$. Results of the calculations are presented in Fig. 2 that demonstrates a good correlation with the analytical result equation (27).

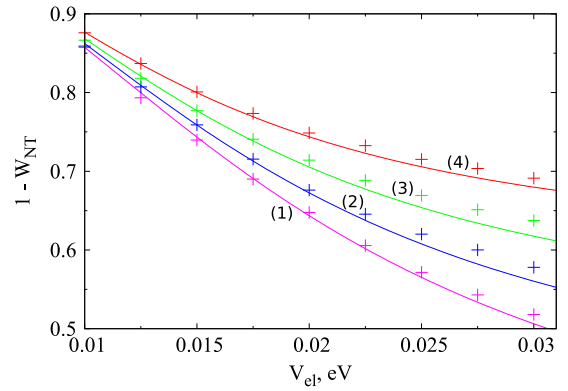


Fig. 2. Plot of survival probability of reagent, $1 - W_{NT}$, as a function of the electronic coupling for several values of the vibrational relaxation time, considering the second vibrational sublevel of the product. The stochastic simulation is pictured with signs +, the exact analytical result is presented by the solid lines. The parameters are: $E_{rm} = 1.0$ eV, $\Delta G = 0.0$ eV, $E_{rv} = 0.3$ eV, $\hbar\Omega = 0.1$ eV, $\tau = 1.0$ ps; (1) $\tau_v = 0.05$ ps, (2) $\tau_v = 0.15$ ps, (3) $\tau_v = 0.5$ ps, (4) $\tau_v = 1000.0$ ps.

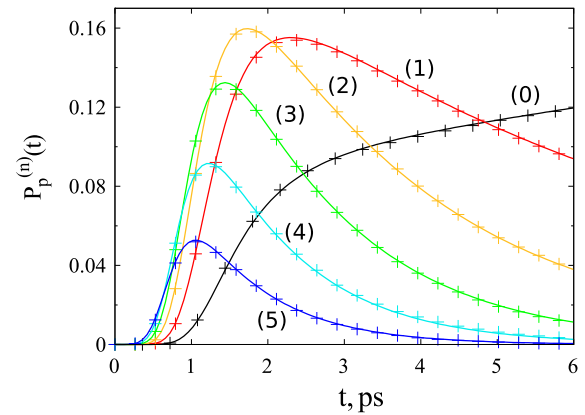


Fig. 3. The time dependence of the product populations for several vibrational sublevels: 0, 1, 2, 3, 4, 5. The stochastic simulation is pictured with signs +, the grid method is presented by the solid lines. The parameters are $V_{el} = 0.01$ eV, $E_{rm} = 1.0$ eV, $\Delta G = -0.5$ eV, $E_{rv} = 0.3$ eV, $\hbar\Omega = 0.1$ eV, $\tau = 1.0$ ps, $\tau_v = 5.0$ ps.

The described comparison is only relevant to the population kinetics of the reactant. To check the correctness of the product kinetics calculation the set of Eqs. (23), (24) has been solved by using the explicit grid method. Finite difference scheme for these equations can be written as follows

$$\frac{\rho_{r,i}^{k+1} - \rho_{r,i}^k}{\Delta t} = A(0) - B(Q_i - Q^*) [\rho_{r,i}^k - \rho_{p,i}^{(n),k}], \quad (28)$$

$$\frac{\rho_{p,i}^{(n),k+1} - \rho_{p,i}^{(n),k}}{\Delta t} = A(\sqrt{2E_{rm}}) + B(Q_i - Q^*) [\rho_{r,i}^k - \rho_{p,i}^{(n),k}] - \frac{n\rho_{p,i}^{(n),k}}{\tau_v}, \quad (29)$$

$$A(Q^*) = \frac{1}{\tau} \left[\rho_{p,i}^{(n),k} + (Q_i - Q^*) \frac{\rho_{p,i+1}^{(n),k} - \rho_{p,i-1}^{(n),k}}{2\Delta Q} + k_B T \frac{\rho_{p,i+1}^{(n),k} - 2\rho_{p,i}^{(n),k} + \rho_{p,i-1}^{(n),k}}{\Delta Q^2} \right], \quad (30)$$

$$B(Q \in [0, \Delta Q]) = \frac{2\pi V_n^2}{\sqrt{2E_{rm}} \Delta Q \hbar}, \quad (31)$$

$$B(Q \notin [0, \Delta Q]) = 0, \quad (32)$$

Table A.1

key	Type	Valid value	Default value	Description
\$MAIN				
numParticles	integer	[10, 2 · 10 ⁹]		The number of particles in a simulation.
particleWeights	real, array	>0.0	[1.0/N, 1.0/N, . . . , 1.0/N]	The weights of particles for simulation processes. Array size is N, where N is the number of program processes.
timeStart	real	≥0.0		Initial time of a simulation.
timeEnd	real	>timeStart		Final time of a simulation.
numTimeLayers	integer	≥10		The number of time layers for a simulation.
numModes_c	integer	≥1		The number of classical relaxation modes.
numModes_v	integer	≥1		The number of quantum vibrational modes.
numTerms	integer	≥2		The number of parabolic terms.
numPairs	integer	≥1		The number of pairs of coupling terms, between which electronic transitions are possible.
hbar	real	>0.0	6.58211928 · 10 ⁻⁴ , eV ps	Plank's constant.
kb	real	>0.0	8.6173303 · 10 ⁻⁵ , eV · K ⁻¹	Boltzmann constant.
T	real	>0.0	300.0	Temperature.
isNewCalculation	integer	0 or 1	1	Specifies a mode of calculation, if value = 1 then initial distribution of particles is generated again, if value = 0 then initial distribution of particles is initialized by the previous calculation.
recordVersion	integer	≥0	0	A number that will be appended to the file name, if value = 0 then *_rv0000.txt, if value = 3 then *_rv0003.txt.
seed	integer	≥ -1	-1	Seed for initialization of PRNG. If value = -1 then initialization depends on system time.
\$MODE_C				
x	real	[0.0, 1.0]		Weight of the solvent mode.
tau	real	>0.0		Relaxation time.
\$MODE_V				
x	real	[0.0, 1.0]		Weight of the vibrational mode.
tau	real	≥0.0		Relaxation time.
omega	real	>0.0		The frequency in the energy units.
numQuantaMax	integer	[0, 20]		The maximum number of quanta of the vibrational mode.
\$TERM				
DeltaG	real	≤0.0		The change in free energy of an electronic term with respect to the reference term. If value = 0 then this term is reference one.
Erm	real	≥0.0		The total reorganization energy of an electronic term with respect to the reference term. If value = 0 then this term is reference one.
\$PAIR				
termsNo	integer, array	[0, numTerms-1]		The indexes of an electronic terms which form a pair. Array size is equal to two.
Vel	real	≥0.0		The electronic coupling between the terms.
Erv	real	≥0.0		The total reorganization energy of high-frequency vibrational modes.
tau	real	≥0.0	0.0	Internal conversion time.
irTermNo	integer	[-1, numTerms-1]	-1	The index of the term with irreversible reaction. If the value = -1 then the reaction is reversible one.
\$SUBTERMS				
mfcLimiter	real	≥0.0	10 ⁻⁹	Subterm associated with the quantum modes is excluded from the manifold, if the product of the Franck–Condon factors of these modes is less than mfcLimiter.
rangeSubterms	integer, array	≥ -1	[-1, -1]	Range of subterms. For example, if the range is [0, 3] then the term includes only 4 subterms from 0 to 3, if the range is [-1, -1] then number of subterms is defined by mfcLimiter.
rangeTransits	integer, array	≥ -1	[-1, -1]	Range of the subterms whose the Franck–Condon factors in the transition point are calculated. The subterms out of the range have the Franck–Condon factors which are equal to 0. For example, if the range is [-1, -1] then all subterms are active. If range is [1, 1] then from all subterms only subterm 1 is active in point-transitions.
\$INITDISTR_THERMAL				
termNo	integer	[0, numTerms-1]		Index of an electronic term with the initial thermal distribution.
Erm	real	≥0.0		The mean value of the initial Gauss distribution is specified by the shifts $\sqrt{2x_iErm}$, the thermal distribution is shifted from its equilibrium position.
\$INITDISTR_PUMP				
pairNo	integer	[0, numPairs-1]		The index of a pair of the terms involved in the excitation by a pump pulse.
termNo	integer	[0, numTerms-1]	The index of the high term from a pair with index pairNo.	The index of the term in the pair where the initial distribution is formed.
tau	real	>0.0		Duration of the pump pulse.

(continued on next page)

Table A.1 (continued)

key	Type	Valid value	Default value	Description
omega	real	>0.0		The carrier frequency of the pump pulse in the energy units.
x_c	real, array	[0.0, 1.0]	Values are specified by \$MODE_Ci.	Weights of component of the reorganization energy of solvent. The array size is equal to numModes_c.
x_v	real, array	[0.0, 1.0]	Values are specified by \$MODE_Vi.	Weights of high-frequency vibrational mode in the total reorganization energy. The array size is equal to numModes_v.
\$KINETICS				
numTimeLayers	integer	[1, numTimeLayers]		The number of time layers to save the populations of the terms and subterms.
numPrintSubterms	integer, array	[1, 100]	[5, 5, ..., 5]	Array size is equal to numTerms. The array elements are the numbers of the subterms whose population is written to the file. The array index is associated with the index of the electronic term and is included in the file name.

where the Dirac delta function is approximated by $B(Q)$. Boundary conditions are $\rho_0^k = \rho_1^k$, $\rho_N^k = \rho_{N-1}^k$, where N is the number of spatial steps.

Calculation are performed with the following parameters: the spatial range of integration is equal to $E_{\text{rm}} = 1.0$ eV, $\Delta G = -0.5$ eV, $V_{\text{el}} = 0.01$ eV, $E_{\text{rv}} = 0.3$ eV, $\hbar\Omega = 0.1$ eV, $\tau = 1$ ps, $\tau_v = 5$ ps. The population kinetics of the product are showed in Fig. 3 for several vibrational sublevels by solid lines. The results of stochastic simulation presented also in Fig. 3 by signs demonstrate excellent coincidence with the grid method.

So, all keys processes implemented in the code have been checked that strongly evidences the code correctness.

6. Concluding remarks

In this work we have presented the `bsmKinetic` code, that implements the stochastic multichannel point-transition approach to simulate charge transfer kinetics in solutions. A detailed description of the use of the code has been provided considering the example of intramolecular photoinduced electron transfer from the second electronic excited state of Zn-porphyrin to imide. The `bsmKinetic` is applicable to the description of the thermal and photoinduced charge transfer kinetics in systems with the reorganization of many intramolecular high-frequency vibrational mode in solvents with several relaxation timescales. It provides simulation of the kinetics in the molecular systems with many electronic states involved in photochemical transformations. Software allows simulating the electron transfer occurring in both equilibrium and nonequilibrium regimes. The nuclear nonequilibrium can be created by both pumping pulse and reaction itself.

The model used has some limitations. The first is connected with the classical description of the solvent fluctuations so that their frequency have to be rather low that requires the inequality $\hbar/\tau_i \ll k_B T$ to be fulfilled for each solvent relaxation mode. The second limitation of the model is caused by description of the vibronic states in terms of populations. This description ignores the quantum coherence and, hence, is applicable if only the electronic coherence lifetime, τ_c , is much shorter than the reaction time constant, $1/k_{\text{et}}$. This results in the inequality $\hbar/\sqrt{2E_{\text{rm}}k_B T} \ll 1/k_{\text{et}}$ [27]. The inequality is met if the electron-solvent interaction is strong and the temperature is high. For $E_{\text{rm}} = 1$ eV and the room temperature this leads to the inequality $k_{\text{et}} \ll 10^{14} \text{ s}^{-1}$. The third limitation is connected with the usage of the diabatic basis. It requires the electronic couplings to be small. Roughly this results in the condition $V_{\text{el}} < k_B T$ [38].

In the current implementation the parabolic approximation of the electronic terms are used. This limitation will be eliminated in future releases. The `bsmKinetic` is hosted in Volgograd State University home page and hence is accessible to all who are willing to get preliminary estimations of the results of planned experiments.

Acknowledgment

The study was performed by a grant from the Russian Science Foundation (Grant No. 16-13-10122).

Appendix. Input keys

See Table A.1.

References

- [1] A.M. Kuznetsov, *Charge Transfer in Physics, Chemistry and Biology*, Gordon & Breach, Amsterdam, 1995.
- [2] R.A. Marcus, N. Sutin, *Biochim. Biophys. Acta* 811 (1984) 265–322.
- [3] W. Domcke, G. Stock, *Adv. Chem. Phys.* 100 (1997) 1–168.
- [4] J. Jortner, M. Bixon (Eds.), *Electron Transfer: from Isolated Molecules to Biomolecules*, in: *Advances in Chemical Physics*, vol. 106, Wiley, New York, 1999, p. 734.
- [5] D.M. Adams, L. Brus, C.E.D. Chidsey, S. Creager, C. Creutz, C.R. Kagan, P.V. Kamat, M. Lieberman, S. Lindsay, R.A. Marcus, R.M. Metzger, M.E. Michel-Beyerle, J.R. Miller, M.D. Newton, D.R. Rolison, O. Sankey, K.S. Schanze, J. Yardley, X. Zhu, *J. Phys. Chem. B* 107 (2003) 6668–6697.
- [6] C. Martín, M. Ziólek, A. Douhal, *J. Photochem. Photobiology C, Photochem. Rev.* 26 (2016) 1–30.
- [7] R. Huber, J.E. Moser, M. Grätzel, J. Wachtveitl, *J. Phys. Chem. B* 106 (2002) 6494–6499.
- [8] B. Oregan, M. Grätzel, *Nature* 353 (1991) 737–740.
- [9] M. Grätzel, *Nature* 414 (2001) 338–344.
- [10] A.I. Burshtein, *Adv. Chem. Phys.* 129 (2004) 105–418.
- [11] E. Vauthey, *J. Photochem. Photobiol. A* 179 (2006) 1–12.
- [12] A.I. Ivanov, V.A. Mikhailova, *Russ. Chem. Rev.* 79 (2010) 1047–1070.
- [13] A. Rosspeintner, B. Lang, E. Vauthey, *Annu. Rev. Phys. Chem.* 64 (2013) 247–271.
- [14] H. Kandori, K. Kemnitz, K. Yoshihara, *J. Phys. Chem.* 96 (1992) 8042–8048.
- [15] Q.H. Xu, G.D. Scholes, M. Yang, G.R. Fleming, *J. Phys. Chem. A* 103 (1999) 10348–10358.
- [16] O. Nicolet, N. Banerji, S. Pagès, E. Vauthey, *J. Phys. Chem. A* 109 (2005) 8236–8245.
- [17] J. Petersson, L. Hammarsröm, *J. Phys. Chem. B* 119 (2015) 7531–7540.
- [18] C. Wan, T. Xia, H.C. Becker, A.H. Zewail, *Chem. Phys. Lett.* 412 (2005) 158–163.
- [19] S.V. Feskov, V.N. Ionkin, A.I. Ivanov, H. Hagemann, E. Vauthey, *J. Phys. Chem. A* 112 (2008) 594–601.
- [20] C. Zimmermann, F. Willig, S. Ramakrishna, B. Burfeindt, B. Pettinger, R. Eichberger, W. Störck, *J. Phys. Chem. B* 105 (2001) 9245–9253.
- [21] C. Ruckebusch, M. Sliwa, P. Pernot, A. de Juan, R. Tauler, *J. Photochem. Photobiology C: Photochemistry Reviews* 13 (2012) 1–27.
- [22] R.G. Fedunov, S.V. Feskov, A.I. Ivanov, O. Nicolet, S. Pagès, E. Vauthey, *J. Chem. Phys.* 121 (2004) 3643–3656.
- [23] A.O. Kichigina, V.N. Ionkin, A.I. Ivanov, *J. Phys. Chem. B* 117 (2013) 7426–7435.
- [24] V.V. Yudanov, V.A. Mikhailova, A.I. Ivanov, *J. Phys. Chem. A* 114 (2010) 12998–13004.
- [25] V.V. Yudanov, V.A. Mikhailova, A.I. Ivanov, *J. Phys. Chem. A* 116 (2012) 4010–4019.
- [26] M.V. Rogozina, V.N. Ionkin, A.I. Ivanov, *J. Phys. Chem. A* 117 (2013) 4564–4573.
- [27] A.E. Nazarov, V.Yu. Barykov, A.I. Ivanov, *J. Phys. Chem. B* 120 (2016) 3196–3205.
- [28] L.D. Zusman, *Chem. Phys.* 49 (1980) 295–304.
- [29] <http://www.gnu.org/licenses/gpl.html>.
- [30] M.V. Rogozina, V.N. Ionkin, A.I. Ivanov, *J. Phys. Chem. A* 116 (2012) 1159–1167.
- [31] M. Maroncelli, V.P. Kumar, A. Papazyan, *J. Phys. Chem.* 97 (1993) 13–17.

- [32] R. Jimenez, G.R. Fleming, P.V. Kumar, M. Maroncelli, *Nature* 369 (1994) 471–473.
- [33] S.V. Feskov, V.N. Ionkin, I.A. Ivanov, *J. Chem. Phys. A* 110 (2006) 11919–11925.
- [34] D.J. Bicout, A. Szabo, *J. Chem. Phys.* 109 (1997) 2325–2338.
- [35] M.L. Horng, J.A. Gardecki, A. Papazyan, M. Maroncelli, *J. Phys. Chem.* 99 (1995) 17311–17337.
- [36] M. Matsumoto, T. Nishimura, *Dynamic Creation of Pseudorandom Number Generators, Monte Carlo and Quasi-Monte Carlo Methods*, 1998, Springer, 2000, pp. 56–69.
- [37] V.A. Mikhailova, A.I. Ivanov, *J. Phys. Chem. C* 111 (2007) 4445–4451.
- [38] A. Barzykin, P. Frantsuzov, K. Seki, M. Tachiya, *Adv. Chem. Phys.* 123 (2002) 511–616.